# Rapid Calcification on Solution Blending of Homogenous PHBV/Collagen Composite

**Wang Yingjun,[1,2] Wu Gang,[1,2] Chen Xiaofen,[1,2] Ye Jiandong,[1,2] Wei Kun[1,2]**

[1]*College of Material Science and Engineering, South China University of Technology, Guangzhou 510640, China*
[2]*Key Laboratory of Specially Functional Materials, Ministry of Education, South China University of Technology, Guangzhou 510640, China*

Received 8 November 2007; accepted 8 October 2008
DOI 10.1002/app.29489
Published online 23 January 2009 in Wiley InterScience (www.interscience.wiley.com).

**ABSTRACT:** Developing of a surface hybrid calcium phosphate-degradable polymer materials is always attractive since it could have high bone bonding ability and proper mechanical properties as natural bone substitute. In this article, a solution blending method was used to make the poly-[(3-hydroxybutyrate)-*co*-(3-hydroxyvalerate)] (PHBV)/collagen composite with high surface calcium apatite deposition capability. Before the blending, the pseudo ternary phase diagram of $CH_3COOH$-$CHCl_3$/PHBV-$H_2O$/collagen at 20°C was plotted. Three compositions selected from the homogenous zone in the diagram were chosen to fabricate the PHBV/collagen composites. Water contact angle, water absorbance ratio, and FTIR spectra showed the collagen contents in the final composites increased with its original blending ratio. The composite with the highest collagen content was chosen for the biomineralization experiment in simulated calcium solution (SCS). Scanning electronic microscopy showed the morphology of the deposition changing from porous structure to plate structure. The FTIR spectra displayed the precipitate was calcium phosphate containing collagen content. The X-ray Diffractometer spectra displayed that the precipitate has the similar characteristic peaks as calcium apatite and the crystalline increased with the biomineralization time. The concentration of calcium and hydrogenphosphate ions in the SCS monitored in the first 4 h decreased to 29.5 and 1.8 ppm, respectively. The Ca/P of the precipitate stabilized at 1.3 in the first 4 h. The FTIR spectra showed that the amide absorption band shifted to low wavelength, which was caused by the electrostatic force between the calcium ions and the amide bond p-π conjugation system. © 2009 Wiley Periodicals, Inc. J Appl Polym Sci 112: 963–970, 2009

**Key words:** PHBV; collagen; solution blending; biomineralization

## INTRODUCTION

Bone is main supporting construction tissue in human body and provides protection for many vital human organs. Though bone possesses strong regeneration capacity, bone substitute materials is still in need when massive bone loss caused by trauma and tumor resection as well as deformities requiring reconstructive surgery.[1,2]

The ideal material for bone substitute should be degradable, non toxic, obtainable material with proper mechanical property and nice osteo-bioactivity. Autograft and allograft bone could be the best choice if they don't have the problems related to availability, diseases/viral transmission, and shaping difficulty.[3,4] Artificial materials were then developed and used for this purpose. They include bioactive glasses,[5,6] calcium hydroxyapatite,[7,8] tricalcium phosphate,[9,10] biphasic calcium phosphate,[11,12] degradable polesters,[13–16] and other polymers. However, they still exist many problems need to be improved to replace and repair the defected bone in body or as the bone tissue engineering scaffold, such as the mechanical properties of the inorganic materials and the bioactivity of polymers.

Biomineralization is a promising way to fabricate bone substitutes. The method uses a selected substrate material as a matrix emerged in a specific liquid to deposit an osteoblast favorite calcium phosphate layer on it. This method avoids the complicate polymer inorganic blending progress. This attractive method can also keep the bulk materials properties without significant influences and get a favorable surface for osteoblast at the same time.

On the polymer surface, it is hypothesized that some anionic groups serve as binding sites for calcium ions and align them in an orientation that matches the apatite crystal lattice.[17–20] Making carboxyl or hydroxyl groups on the surface will benefit the biomineralization processing on it, like those

*Correspondence to:* W. Gang (imwugang@scut.edu.cn).
Contract grant sponsor: National Science Foundation of China; contract grant number: 50403023.
Contract grant sponsor: 973 project in China; contract grant number: 2005CB623902.

have been done on the PLA,[21] PLGA,[22] PGA,[23] and PCL[24] surface.

PHBV is a promising biodegradable polyester synthesized by the microorganisms and/or plants.[25,26] Its high mechanical property, tailorable degradability, special piezoelectricity benefit bone's regeneration, and the nontoxicity of both the material and degraded products make it a promising biopolymer for bone substitute and bone tissue engineering.[27–29] However, PHBV lacks biomineralization and osteoactive groups as all degradable polyesters. Furthermore, the osteoblast unfavorable hydrophobic surface limits its application.[30–32]

Collagen is reported as a tissue favorable natural material and used as biomedical material for long times. It is the main organic part of bone. Blending collagen with PHBV is hoped to improve the biomineralization ability and bioactivity of PHBV.

Although the successful extrusion blending of PHBV with natural polymers have been reported, such as the starch,[33] wood fiber,[34] wheat straw fiber,[35] pineapple fiber,[36] and many other kinds of fibers,[37–40] mild blending approach is preferable since the collagen denaturation temperature is far lower than the extrusion processing temperature. Room temperature solution blending can avoid that and keep the bioactivity of collagen.

However, phase separation existing between hydrophobic PHBV and hydrophilic collagen solutions prevents homogenous blending of them and few papers could be found. In this article, we studied the ternary phase diagram needed for the homogenously solution blending to produce PHBV/collagen composites. Furthermore, the calcification capability of such composite was studied.

## MATERIALS AND METHODS

### Materials

PHBV (20% HB content) was purchased from American Metalolix Inc, (Cambridge, MA). PHBV/chloroform solution (150 mg/100 mL) was prepared before experiment. Bovine Type I collagen solution (6.5 mg/L) was purchased from Chuanger biotechnology, China, and used as received. Other chemical reagents including chloroform, $K_2HPO_4$, KCl, NaCl, $CaCl_2$, HCl, and tris(hydroxymethyl)aminomethane (Tris) was purchased from Sigma and used as received.

### Solution blending of PHBV/collagen composite

Before the solution blending, a ternary phase diagram at room temperature (20°C) was plotted as the following steps. Nine different acetic acid-PHBV chloroform solution mixtures were prepared with the chloroform/acetic acid molar ratio of 1.0, 0.9, 0.8, 0.7, 0.6, 0.5, 0.4, 0.3, and 0. Another six acetic acid-collagen mixtures were also prepared with the water/acetic acid molar ratio of (9 : 0.02), (8 : 0.05), (7 : 0.08), (6 : 0.12), (5 : 0.16), and (4 : 0.22). Titrate the acetic acid-PHBV chloroform solutions and acetic acid-collagen solutions with water and chloroform, respectively, until a two phase system is formed. Calculate the molar fractions and plot the results of the titrations in a triangular diagram.

Three points inside the homogeneous zone in the ternary diagram were selected with the volume ratio (PHBV chloroform solution : acetic acid : collagen solution) of 1 : 5 : 4, 1 : 2 : 1, and 4 : 5 : 1, respectively. The mixture solutions were stirred for 30 min and debubble for 10 min under vacuum. Then, they were frozen in the liquid nitrogen and lyophilized in a frieze dryer (Christ, alpha 2–6). Finally, the lyophilized composite was extracted by the deionized water and vacuum dried for 1 day before using.

### Biomineralization on the composites surface

SCS was prepared as the reported literature.[41] The final ions concentrations in SCS as reported were $K^+$: $4.646 \times 10^{-3}$ mol/L, $Na^+$: 0.1374 mol/L, $Ca^{2+}$: $3.225 \times 10^{-3}$ mol/L, $Cl^-$: 0.1390 mol/L, and $HPO_4^{2-}$: $1.860 \times 10^{-3}$ mol/L. The composites were immerged in 50 mL SCS in a sealed 100-mL plastic bottles and incubated in a 37.5°C oven for 4 days. The solution was replaced every day. The calcium and hydrogenphosphate ions in SCS were analyzed every half hour in the first 4 h by ions chromatography. The precipitates on the composite surface at the 4th hour and after the experiment were carefully separated, collected, and analyzed by FTIR and X-ray Diffractometer (XRD). Samples of the composite were taken and characterized by Scanning electronic microscope (SEM) and FTIR after biomineralization.

### Water contact angle

Static water contact angle measurements were carried out by the water contact measure meter equipped with CCD detector, dosing control system and related software (CA10 + OCA20, Dataphysics, German). Sessile drop method was used here with concisely controlled dosing water volume of 1 μL every time. All contact angles were the means of five measurements on different parts of the irradiated spot ± standard error (SE).

### Water absorbance ratio

The composite with the weight of $W_0$ was put into distilled water and taken out 3 h later. After absorbing the water on the surface, it was weighted again

($W_1$). The water absorbance ratio was calculated as following equation:

$$\mathrm{WAR}(\%) = \frac{W_1 - W_0}{W_0} \times 100$$

### Ions chromatography

Dionex D×600 chromatography (Sunnyvale, CA) equipped with quaternary gradient pump (GS50), chromatography module (LC30), and detector module (ED50) worked in the recycle mode at the constant temperature of 30°C and controlled by Chromeleon 6.40 software. Columns used were Dionex IonPac CG12A, CS12A, AG7, AS7, and ATLAS Electrolytic Suppressor columns according to cation or anion, respectively. The sample-loop volume was 25 μL. Calibration was performed with the standard solution of $Na_2HPO_4$ and $CaCl_2$.

An estimated Ca/P ratio of the precipitate was calculated according to the following equation:

$$\mathrm{Ca/P} = \frac{[\mathrm{Ca}]_0 - [\mathrm{Ca}]_t}{[\mathrm{P}]_0 - [\mathrm{P}]_t}$$

$[Ca]_0$ and $[P]_0$ are the original concentration of calcium and hydrogenphosphate in the solution, and $[Ca]_t$ and $[P]_t$ are the measured ion concentration at different times.

### SEM

Scanning electronic microscopy (Philips, XL30) was used to observe the surface morphology after experiments. The sample was taken out from the SCS and dried in a 37.5°C oven for 1 day. Then it was sputtering coated (E-1010, Hitachi, Japan) with Au for morphology observing.

### FTIR

Infrared spectra of those collected precipitates were collected using a FTIR spectrometer (Nicolet 670, Thermo) equipped with the apparatus for attenuated total reflection (ATR) measurements (IRE: germanium) by KBr pellet method. A mercury cadmium telluride (MTC) detector was used and 64 scans were collected between 4000 $cm^{-1}$ and 400 $cm^{-1}$ with the resolution of 1 $cm^{-1}$.

### XRD

The collected calcium phosphate powder was stacked on the glass surface. The crystalline phases of the HA powders was determined by an X-ray Diffractometer (XRD, X'pert Pro, PANlytical, Netherland) using Cu Kα radiation, with a step of 0.03° and at a speed of 4° per minute.

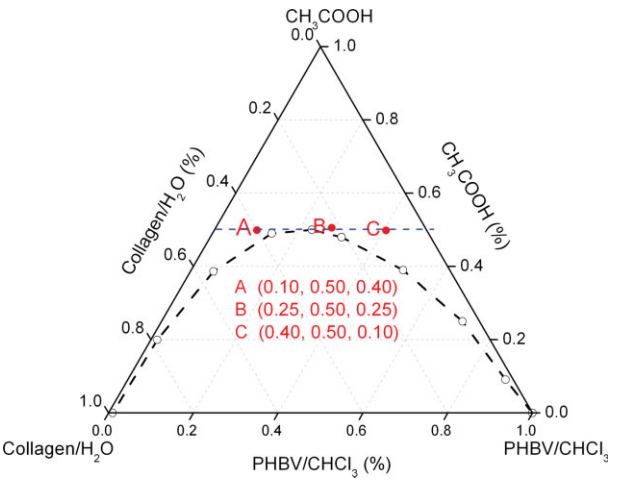


**Figure 1** Pseudo ternary phase diagram of $CH_3COOH$-collagen solution-PHBV chloroform solution (20°C). [Color figure can be viewed in the online issue, which is available at www.interscience.wiley.com.]

## RESULTS AND DISCUSSION

### Ternary diagram of pseudo acetic acid-PHBV solution-collagen solution

Figure 1 is the ternary phase diagram of acetic acid, water/collagen, and chloroform/PHBV. In this diagram, the homogenous zone is above the immiscibility boundaries, whereas below that curve is the phase split zone. Three points A, B, and C inside the homogenous zone is selected for the solution blending experiment with the volume ratio ($CHCl_3$/PHBV : $CH_3COOH$ : $H_2O$/Collagen) of (1 : 5 : 4), (1 : 2 : 1), and (4 : 5 : 1), respectively. Since acetic acid can mix with both chloroform and water, the existence of it definitely decreases the surface tension between chloroform and water when they were mixed together and makes it possible to get a homogenous zone within a range of ratio. Because the mixing was carried out under room temperature, the collagen denature would be prevented during this process.

### Solution blending of PHBV/collagen composites

Figure 2 displays the water contact angle and water absorption ratio of different PHBV/collagen composites. In the figure, the water contact angle decreased with the collagen content increasing in those composites, whereas the water absorption ratio increased with that. Since collagen is more hydrophilic than PHBV, collagen content increasing in composites definitely improved the hydrophilicity of those

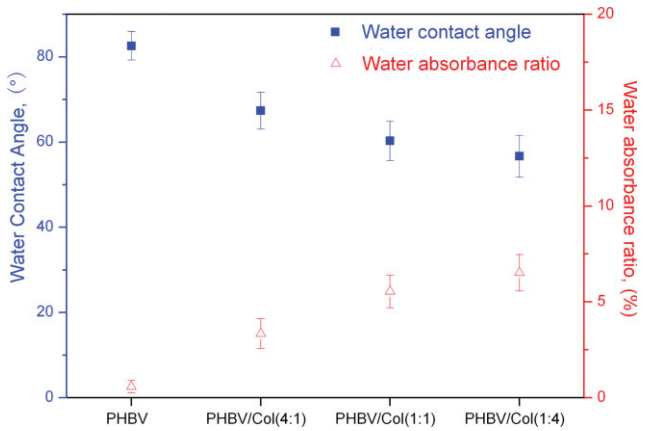


**Figure 2** Water contact angle and absorption ratio after of the PHBV/collagen composite. [Color figure can be viewed in the online issue, which is available at www.interscience.wiley.com.]

blending composites. Furthermore, the increasing of surface polarity will decrease the composites' surface energy benefiting organic substrate-mineral nucleus interface and promoting the mineral formation on the polymer substrates.[42]

Figure 3 shows the FTIR spectra of the PHBV/collagen composites with the volume ratio of A, B, and C after blending. The absorption bands at 3434.57 $cm^{-1}$, 2975.70 $cm^{-1}$/2937.06 $cm^{-1}$, and 1724.64 $cm^{-1}$ are assigned to hydroxyl, alkyl, and carboxyl groups' distinct absorption bands of PHBV. While the absorption bands at 1652.17 $cm^{-1}$ and 1543.48 $cm^{-1}$ are assigned to the collagen amide I and II distinct absorption bands.

From Figure 3, same regular can be found as that in Figure 2. The results indicate that the collagen content in the composite increased with the initial mixing proportion. With the increasing of the collagen blending ratio, the strength of amide absorption band increased and the hydroxyl absorption band at 3434.57 $cm^{-1}$ became wider due to the existence of strong hydrogen bond inside collagen molecular. The strength of the carboxyl absorption band at 1724.64 $cm^{-1}$, mainly belongs to PHBV, decreased with the decreasing of the PHBV content. Phase separation is not significant and homogeneous blending of PHBV/collagen composite with expected composition can be fabricated through this method.

## Biomineralization on the PHBV/collagen matrix

PHBV/collagen composite of Group C was selected and used for biomineralization experiment since collagen content is higher and it is supposed to have the best biomineralization capability.

Figure 4 shows the morphology of those precipitated calcium phosphate on the PHBV/collagen matrix surface at different biomineralization time. Before mineralization, the surface of PHBV/collagen composite displayed in Figure 4(a) is smooth. Precipitates began to appear on the surface after the first half hour [arrow points in Fig. 4(b)]. More and more such porous and ridge-like precipitate structures perpendicular to the surface were presented on the composites' surface with the increasing of biomineralization time in the first 4 h [Fig. 4(b–e)]. But after 4 days biomineralization, only regular plates with high stacking density forming a hemisphere structures were observed on the polymer surface [Fig. 4(f)]. It is also found that the morphology changing happened in this article, whereas only precipitates amount increasing were found in other works.[21–24] Since PHBV molecular is quite similar to those PLA and PLGA, the morphology changing in Figure 4 should be the reason of collagen's adding. The chemical compositions of the precipitates were studied by FTIR and XRD in the following paragraph.

Figure 5 displays the FTIR spectra of the precipitate at 4 h and 4 days, respectively. 3465.22 $cm^{-1}$ is the absorption band of collagen hydroxyl group, 1656.43 $cm^{-1}$ and 1545.48 $cm^{-1}$ belong to collagen amide I and II absorption band, 1721.74 $cm^{-1}$ is the C=O stretching vibration of PHBV carboxyl group, 1258.14 $cm^{-1}$, 1094.78 $cm^{-1}$ is the P=O stretching vibration, 1034.78 $cm^{-1}$ belongs to P—O stretching vibration band, 600.00 $cm^{-1}$ and 566.87 $cm^{-1}$ belongs to P—O bending vibration band. The spectrum of precipitate of 4 h biomineralized in SCS displays the deposition with calcium phosphate characteristics was observed. The collagen content was also found inside this precipitate. That indicates that collagen was involved in biomineralization

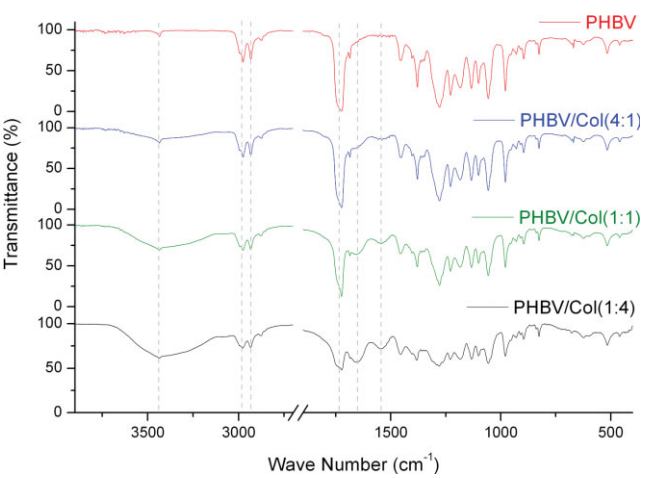


**Figure 3** FTIR spectra of PHBV/collagen composites with different blending ratio. [Color figure can be viewed in the online issue, which is available at www.interscience.wiley.com.]

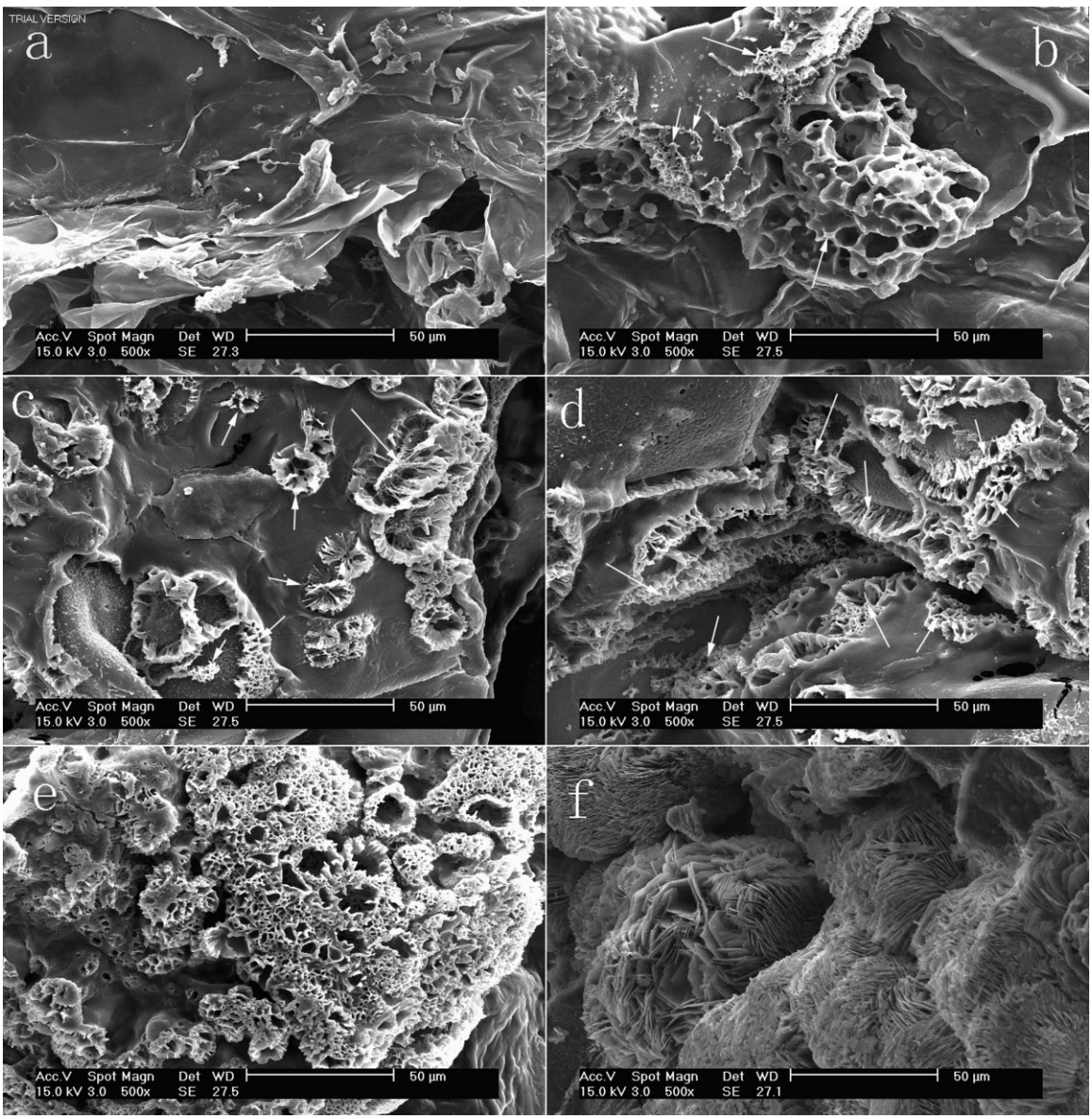


**Figure 4** Morphology of the deposited calcium phosphate at the different biomineralization time (a: 0 h, b: 0.5 h, c: 1 h, d: 2 h, e: 4 h, and f: 4 days).

causing the morphology change in the process. The FTIR spectrum of the precipitate at 4 days shows that the collagen content was largely decreased comparing to the 4 h and more calcium phosphate content inside the precipitate were observed. With the decreasing of collagen content, the morphology is more close to those found in other papers.[21–24]

Figure 6 is the XRD spectra of the precipitate at the fourth hour and the fourth day. The spectrum of the deposition at the fourth hour, with disperse and wide peaks, displays low crystallite deposition formed on the surface. The crystallite was improved at day 4 since the typical peaks belonging to HA/OCP become sharper as that shown in Figure 6.

The precipitate structures were transformed from less crystalline at the first several hours to crystal plates after 4 days biomineralization (Figs. 4–6). In natural bone synthesis, it is suggested that the biomineralization process starts with the formation of poorly crystalline calcium apatite, which are then modified through crystalline phase transitions to form the more stable mature bone apatite with increased crystallinity.[43] In this article, during the biomineralization procedure, the similar crystalline structure formation and transformation was observed. The precipitated calcium phosphate transform from high collagen content and less crystalline to less collagen content and high crystalline state. This suggests that the nucleus of the calcium phosphate was happened on the collagen molecules followed with crystal transformation and growth inside the deposited calcium phosphate clusters.

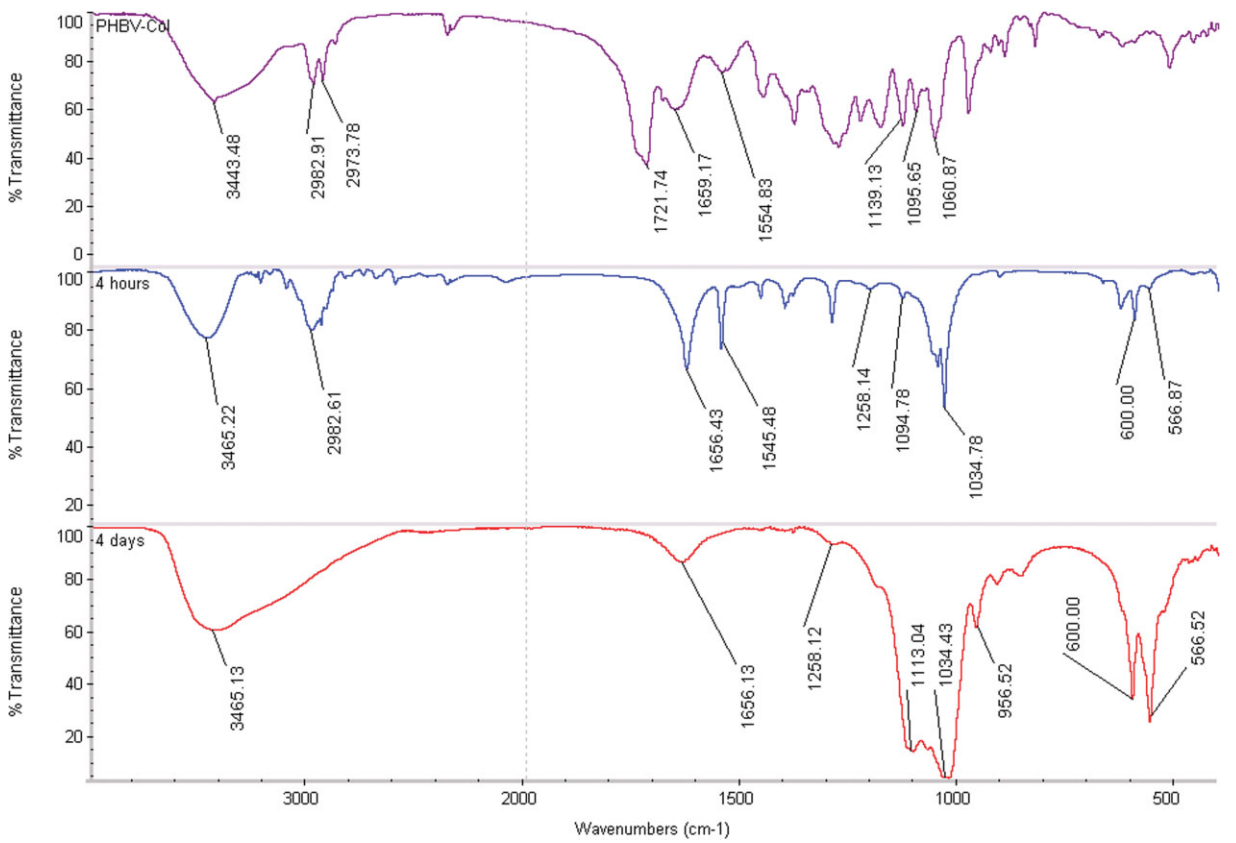


**Figure 5** FTIR spectra of the precipitate at 4 h and 4 days. [Color figure can be viewed in the online issue, which is available at www.interscience.wiley.com.]

### Changes of the ions concentration in SCS

Figure 7 displays changes of the calcium and phosphate ions concentration in solution and the change of the estimated precipitate Ca/P ratio in the first 4 h. Both the ion concentration of calcium and hydrogenphosphate decreased in the period. Especially in the first 1 h, the decreasing was faster than all the other times. Then, the decreasing became slowly. The ions precipitation behavior in SCS is different from each other. The hydrogenphosphate ions kept on precipitating from SCS during the fourth hour, whereas the calcium ions mainly precipitate in the first one and a half hours.

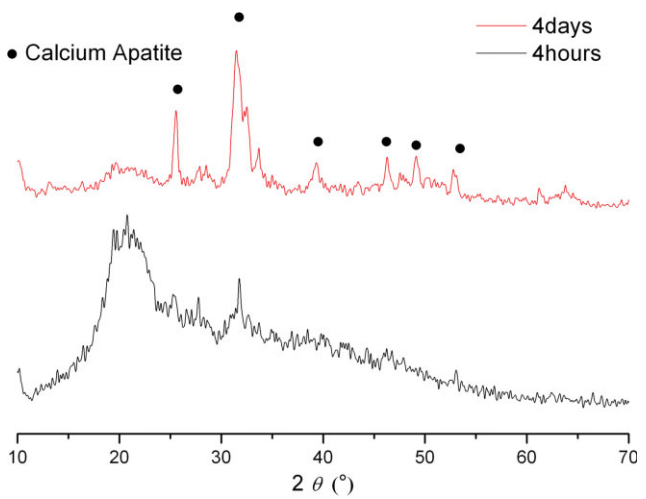


**Figure 6** XRD spectra of the precipitate at 4 h and 4 days. [Color figure can be viewed in the online issue, which is available at www.interscience.wiley.com.]

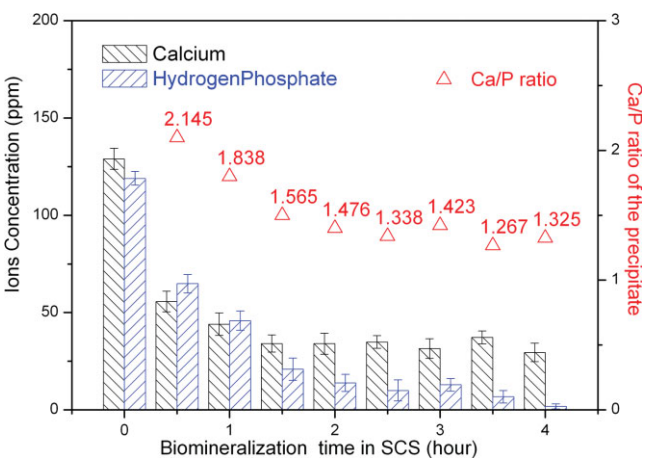


**Figure 7** Change of the ions' concentration in the SCS and the Ca/P ratio of the precipitate in first 4 h. [Color figure can be viewed in the online issue, which is available at www.interscience.wiley.com.]

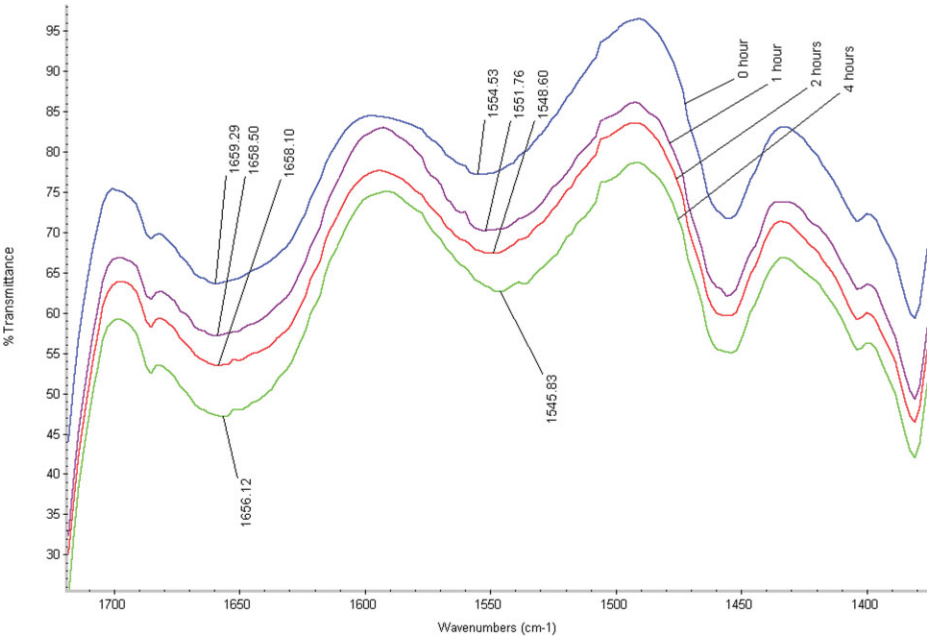


**Figure 8** Shift of amide I and II caused by the electrostatic force between them and calcium cations. [Color figure can be viewed in the online issue, which is available at www.interscience.wiley.com.]

The faster decreasing of calcium in the first hour shows that the calcium is the main deposition on the matrix during this period. This fast calcium deposition could be the reason for the amorphous calcium phosphate presented on the SEM since the high speed deposition influence the crystal's normal growth on the matrix surface.

The Ca/P ratio of the precipitate also decreased along with the composite soaking time and stabilized at 1.3. The Ca/P shows that the deposition of the calcium in the solution is faster than that of hydrogenphosphate especially in the first 1 h. That means in the first hour, the main interaction is between the calcium and collagen.

### Interaction between calcium phosphate and collagen

Figure 8 displays the shift of the amide I and II distinct absorption band during the initial 4 h biomineralization. They shifted from original positions of 1659.29 $cm^{-1}$ and 1554.53 $cm^{-1}$ to final positions of 1656.12 $cm^{-1}$ and 1545.83 $cm^{-1}$. Amide I shifted to long wavelength 3 $cm^{-1}$ and amid II shifted 9 $cm^{-1}$. This shifting could be the reason of electrostatic force between the calcium ion and the amide group. The amide bond has a p-π conjugation structure with high electron cloud density. The interaction between the calcium cations and this conjugation structure lead to a transformation of the p-π conjugation structure and decreased the electron cloud density. Therefore, the amide absorption bands move to the long wave length. This displays the nuclei positions for the calcium phosphate could be also happened at the sites of collagen amide groups.

The calcium phosphate deposition on the collagen matrix was, as hypothesized in the literature,[44] attributed to the electrostatic force interaction between the cations and the anionic whole zone of the collagen along with the structural and stereochemical interactions. The calcium-rich mineral nuclei were attracted in this whole zone and then the mineral growth initiated. In this article, not only the whole zone, but also the amide content play a role in the biomineralization process.

## CONCLUSIONS

In this article, three PHBV/collagen composites with different composition had been successfully fabricated through solution blending method. The pseudo ternary phase diagram of $CH_3COOH$-PHBV chloroform solution-collagen solution was got. According to this diagram, three homogenous PHBV/collagen composites with different mix ratio were made through solution blending. The FTIR, water contact angle, and water absorbance ratio results displayed the collagen contents in the final composites related to its original mixing ratio.

The interaction between the collagen and the solution ions is the reason for the calcium phosphate deposition on the PHBV/collagen composite surface. The precipitate transformed from less crystalline calcium apatite with high collagen content to high crystalline with less collagen content.

The PHBV/collagen composite shows good biomineralization property *in vitro* in this article. Considering the nice cell compatibility of the collagen content, this composite could be a promising bone substitute and bone tissue engineering scaffold material.

## References


1. Mistry, A. S.; Mikos, A. G. Adv Biochem Eng Biotechnol 2005, 94, 1.
2. Hoexter, D. L. J Oral Implantol 2002, 28, 290.
3. Capanna, R.; Campanacci, D. A.; Belot, N.; Beltrami, G.; Manfrini, M.; Innocenti, M.; Ceruso, M. Orthop Clin North Am 2007, 38, 51.
4. Eppley, B. L.; Pietrzak, W. S.; Blanton, M. W. J Craniofac Surg 2005, 16, 981.
5. Oonishi, H.; Hench, L. L.; Wilson, J.; Sugihara, F.; Tsuji, E.; Matsuura, M.; Kin, S.; Yamamoto, T.; Mizokawa, S. J Biomed Mater Res 2000, 51, 37.
6. Yuan, H.; De Bruijn, J. D.; Zhang, X.; Van Blitterswijk, C. A.; De Groot, K. J Biomed Mater Res 2001, 58, 270.
7. Ozawa, S.; Kasugai, S. Biomaterials 1996, 17, 23.
8. Yoshikawa, H.; Myoui, A. J Artif Organs 2005, 8, 131.
9. Kotani, S.; Fujita, Y.; Kitsugi, T.; Nakamura, T.; Yamamuro, T.; Ohtsuki, C.; Kokubo, T. J Biomed Mater Res 1991, 25, 1303.
10. Neo, M.; Herbst, H.; Voigt, C. F.; Gross, U. M. J Biomed Mater Res 1997, 39, 71.
11. Boden, S. D.; Martin, G. J.; Morone, M. A.; Ugbo, J. L. Spine 1999, 24, 1179.
12. Kivrak, N.; Tas, A. C. J Am Ceram Soc 1998, 81, 2245.
13. Saito, N.; Murakami, N.; Takahashi, J.; Horiuchi, H.; Ota, H.; Kato, H.; Okada, T.; Nozaki, K.; Takaoka, K. Adv Drug Deliv Rev 2005, 57, 1037.
14. Coombes, A. G. A.; Meikle, M. C. Clin Mater 1994, 17, 35.
15. Jagur-Grodzinski, J. Polym Adv Technol 2006, 17, 395.
16. Gomes, M. E.; Reis, R. L. Int Mater Rev 2004, 49, 261.
17. Bajpai, A. K.; Singh, R. Polym Int 2007, 56, 557.
18. Yin, Y. J.; Luo, X. Y.; Cui, J. F.; Wang, C. Y.; Guo, X. M.; Yao, K. D. Macromol Biosci 2004, 4, 971.
19. Lin, J.; Gates, E.; Bianconi, P. A. J Am Chem Soc 1994, 116, 4738.
20. Kretlow, J. D.; Mikos, A. G. Tissue Eng 2007, 13, 927.
21. Zhang, R.; Ma, P. X. Macromol Biosci 2004, 4, 100.
22. Murphy, W. L.; Mooney, D. J. J Am Chem Soc 2002, 124, 1910.
23. Schwarz, K.; Epple, M. Chem—A Eur J 1998, 4, 1898.
24. Seregin, V. V.; Coffer, J. L. Biomaterials 2006, 27, 4745.
25. Keeler, R. R D: Res Dev Kobe Steel Eng Rep 1991, 33, 27.
26. Köse, G. T.; Korkusuz, F.; Ozkul, A.; Soysal, Y.; Ozdemir, T.; Yildiz, C.; Hasirci, V. Biomaterials 2005, 26, 5187.
27. Torun, K.; Korkusuz, F.; Korkusuz, P.; Purali, N.; Ozkul, A.; Hasirci, V. Biomaterials 2003, 24, 4999.
28. Misra, S. K.; Valappil, S. P.; Roy, I.; Boccaccini, A. R. Biomacromolecules 2006, 7, 2249.
29. Yagmurlu, M. F.; Korkusuz, F.; Gürsel, I.; Korkusuz, P.; Ors, U.; Hasirci, V. J Biomed Mater Res 1999, 46, 494.
30. Chen, L. J.; Wang, M. Biomaterials 2002, 23, 2631.
31. Jones, J. R.; Hench, L. L. Mater Sci Technol 2001, 17, 891.
32. Kokubo, T.; Kim, H. M.; Kawashita, M. Biomaterials 2003, 24, 2161.
33. Avella, M.; Errico, M. E.; Rimedio, R.; Sadocco, P. J Appl Polym Sci 2002, 83, 1432.
34. Singh, S.; Mohanty, A. K. Compos Sci Technol 2007, 67, 1753.
35. Avella, M.; La Rota, G.; Martuscelli, E.; Raimo, M.; Sadocco, P.; Elegir, G.; Riva, R. J Mater Sci 2000, 35, 829.
36. Luo, S.; Netravali, A. N. Polym Compos 1999, 20, 367.
37. Bhardwaj, R.; Mohanty, A. K.; Drzal, L. T.; Pourboghrat, F.; Misra, M. Biomacromolecules 2006, 7, 2044.
38. Teramoto, N.; Urata, K.; Ozawa, K.; Shibata, M. Polym Degrad Stab 2004, 86, 401.
39. Luo, S.; Netravali, A. N. J Adhes Sci Technol 2001, 15, 423.
40. Buzarovska, A.; Bogoeva-Gaceva, G.; Grozdanov, A.; Avella, M.; Gentile, G.; Errico, M. J Mater Sci 2007, 42, 6501.
41. Wen, H. B.; Moradian-Oldak, J.; Zhong, J. P.; Greenspan, D. C.; Fincham, A. G. J Biomed Mater Res 2000, 52, 762.
42. Mann, S.; Ozin, G. A. Nature 1996, 382, 313.
43. Song, J.; Saiz, E.; Bertozzi, C. R. J Am Chem Soc 2003, 125, 1236.
44. Wen, H. B.; Moradian-Oldak, J.; Zhong, J. P.; Greenspan, D. C.; Fincham, A. G. J Biomed Mater Res 2000, 52, 762.